



**HAL**  
open science

## Extreme Enhancement of Carbon Hydrogasification via Mechanochemistry

Gao-feng Han, Peng Zhang, Pascal Scholzen, Hyuk-jun Noh, Mihyun Yang,  
Do Hyung Kweon, Jong-pil Jeon, Young Hyun Kim, Seong-wook Kim,  
Sun-phil Han, et al.

► **To cite this version:**

Gao-feng Han, Peng Zhang, Pascal Scholzen, Hyuk-jun Noh, Mihyun Yang, et al.. Extreme Enhancement of Carbon Hydrogasification via Mechanochemistry. *Angewandte Chemie*, 2023, 61 (18), 10.1039/D1CP05164D . hal-03793668v2

**HAL Id: hal-03793668**

**<https://hal.science/hal-03793668v2>**

Submitted on 1 Oct 2022

**HAL** is a multi-disciplinary open access archive for the deposit and dissemination of scientific research documents, whether they are published or not. The documents may come from teaching and research institutions in France or abroad, or from public or private research centers.

L'archive ouverte pluridisciplinaire **HAL**, est destinée au dépôt et à la diffusion de documents scientifiques de niveau recherche, publiés ou non, émanant des établissements d'enseignement et de recherche français ou étrangers, des laboratoires publics ou privés.



Distributed under a Creative Commons Attribution 4.0 International License

# Extreme Enhancement of Carbon Hydrogasification via Mechanochemistry

Gao-Feng Han<sup>1</sup>, Peng Zhang<sup>2\*</sup>, Pascal Scholzen<sup>3</sup>, Hyuk-Jun Noh<sup>1</sup>, Mihyun Yang<sup>4</sup>, Do Hyung Kweon<sup>1</sup>, Jong-Pil Jeon<sup>1</sup>, Young Hyun Kim<sup>1</sup>, Seong-Wook Kim<sup>1</sup>, Sun-Phil Han<sup>5</sup>, Andrey S. Andreev<sup>6</sup>, Guillaume Lang<sup>7</sup>, Kyuwook Ihm<sup>4</sup>, Feng Li<sup>1</sup>, Jean-Baptiste d'Espinose de Lacaillerie<sup>3\*</sup> and Jong-Beom Baek<sup>1\*</sup>

<sup>1</sup>*School of Energy and Chemical Engineering/Center for Dimension-Controllable Organic Frameworks, Ulsan National Institute of Science and Technology (UNIST), 50 UNIST, Ulsan 44919, South Korea.*

<sup>2</sup>*Laboratory for Water Quality and Conservation of the Pearl River Delta, Ministry of Education, Institute of Environmental Research at Greater Bay, Guangzhou University, Guangzhou 510006, P. R. China.*

<sup>3</sup>*Soft Matter Science and Engineering Laboratory (SIMM), UMR CNRS 7615, Université PSL, ESPCI Paris, Paris, France.*

<sup>4</sup>*Pohang Accelerator Laboratory, Pohang 37673, South Korea.*

<sup>5</sup>*UNIST Central Research Facilities, Ulsan National Institute of Science and Technology (UNIST), Ulsan 44919, South Korea.*

<sup>6</sup>*TotalEnergies One Tech Belgium (TEOTB), Zone Industrielle C, 7181, Feluy, Belgium*

<sup>7</sup>*LPEM, ESPCI Paris, PSL University, Sorbonne Université, CNRS, 75005 Paris, France*

\*e-mail: [jbbaek@unist.ac.kr](mailto:jbbaek@unist.ac.kr); [jean-baptiste.despinose@espci.fr](mailto:jean-baptiste.despinose@espci.fr) (J.-B.d.L.); [pengzhang85@foxmail.com](mailto:pengzhang85@foxmail.com) (P.Z.)

**Abstract:** Carbon hydrogasification is the slowest reaction among all carbon-involved small molecule transformations. Here, we demonstrate a mechanochemical method that results in both a faster reaction rate and a new synthesis route. The reaction rate was dramatically enhanced by up to 4 orders of magnitude compared to the traditional thermal method. Simultaneously, the reaction exhibited a very high selectivity (99.8% CH<sub>4</sub>, versus 80% under thermal conditions) with a cobalt catalyst. Our study demonstrated that this extreme increase in reaction rate originates from the continuous activation of reactive carbon species via mechanochemistry. The high selectivity is intimately related to the activation at low temperature, at which higher hydrocarbons are difficult to form. This work is expected to advance studies of carbon hydrogasification, and other solid-gas reactions.

## MAIN TEXT

### Introduction:

Carbon hydrogasification (CHG) is widely used in important industrial applications including hydrocarbon synthesis, coal/biomass gasification,<sup>[1]</sup> and exhaust gas treatment.<sup>[2]</sup> It is also involved in tailoring the growth of graphene,<sup>[3]</sup> and more importantly, in regenerating catalysts deactivated by coke in many carbon-involved reactions — such as the reactions involved in plastic downcycling<sup>[4]</sup> and petroleum refining,<sup>[5]</sup> the water-gas shift reaction,<sup>[6]</sup> the steam reforming reaction,<sup>[7]</sup> and the Fischer-Tropsch reaction.<sup>[8]</sup> However, CHG is a particularly slow reaction, even at practical operating temperatures (at least 450 °C).<sup>[1,9]</sup> For example, the CHG rate is 8 orders of magnitude slower than the carbon oxidation reaction.<sup>[1,9]</sup> This poor performance is due to the following paradoxical facts. The C–C bond has a very high energy barrier (7.4 eV at zigzag edges).<sup>[10]</sup> Consequently, the release of C atoms from the carbon matrix requires high temperature activation. However, CHG is an exothermic reaction. According to Le Chatelier's principle, a low temperature is thus favorable from the viewpoint of reaction equilibrium. Overcoming this dilemma is a big challenge.

In the scientific community, ball-milling is frequently applied as a technique to realize high-temperature reactions at low temperature.<sup>[11,12]</sup> It also has already been used to activate carbon materials and to create very reactive carbon species due to the formation of dangling carbon bonds.<sup>[13–15]</sup> Those unique applications of ball-milling give us a clue to solve the above problem.

In this study, we avoided the thermodynamically constrained CHG by using a mechanochemistry method. The raw carbon materials were activated by ball-milling, and the activated carbon was quickly hydrogenated on the catalyst surface even at ambient temperature (25 °C). The mechanical movement guaranteed that the carbon remains in close contact with the catalyst at all times. The rate of reaction at 40 °C using our method was boosted by as much

as 4 orders of magnitude compared to the traditional thermal method at 600 °C. Remarkably, the reaction also showed very high selectivity [99.8% CH<sub>4</sub>, versus 80% under thermal conditions at equilibrium state (600 °C)], due to the thermally favorable driving force at low temperature. Our studies determined that the continuous formation of mechanochemically induced carbides contributed to the extreme improvement in reaction rate. Our work is thought to open a new approach for direct hydrocarbon synthesis and nonoxidative catalyst regeneration without aggregation at low temperature.

## Results and Discussion:

The CHG was accomplished using a commercially available ball-milling device. In short, the raw carbon materials and metal granules (which acted as catalyst) were loaded into a ball-milling container and sealed in a glovebox protected by argon (Ar). After the container was taken out of the glovebox, it was charged with hydrogen gas. Since commercial metal granules were directly used as catalyst, an *in-situ* nanosizing pretreatment was conducted prior to further study. The hydrocarbon products were checked by gas chromatography (GC).

Before carrying out experiments, to rule out possible interferences, a blank experiment without metal catalysts was performed. The gas was charged/discharged with a home-made gas line, which can eliminate possible gas contamination (Figure S1). As shown in Figure S2, only negligible hydrocarbons were generated. The yield rate (per time unit) without catalyst was at least 4 orders of magnitude lower than that with the catalyst.

Our experiment indicated that cobalt (Co) was the most active catalyst for CHG amongst iron (Fe), Co, nickel (Ni), and copper (Cu) (Figure S3, S4). Interestingly, the activity trends were different from those observed with the traditional thermal method, where Ni is considered to be the best catalyst.<sup>[16,17]</sup> The difference indicates that the mechanochemistry approach relies on a completely new reaction pathway, which is distinct from the traditional thermal method. A distinctive scientific scenario is thought to occur due to the unique nonequilibrium properties of mechanochemistry, which include high density defects and violent impacts (*vide infra*).<sup>[11]</sup>

Another interesting phenomenon is that the activity was found to depend on the type of carbon used (Figure S5a). The level of activity followed the order: charcoal > carbon black > graphite. The activity was thus inversely related to the crystallinity of the C source (Figure S5b), suggesting that a low crystallinity made dissociation easier. Furthermore, this dependence on crystallinity implied that the carbon dissociation step contributes strongly to the overall CHG reaction. Nevertheless, in this work, we selected carbon black rather than charcoal to study the general reaction kinetics because natural wood-derived charcoal contains high levels of impurities.

Co catalyst and carbon black were selected as the typical combination for studying the reaction kinetics. The ratio of Co catalyst (25.3 g) to carbon black (3 g) showed the highest CH<sub>4</sub> yield (Figure S6a). Our experiments indicated that the reaction rate in the measured region monotonically increased as the rotation speed increased (Figure S6b). The reaction rate of CHG was high in the beginning, then declined as the reactive carbon species were consumed (Figure S6c, d). To compare activity, we opted for the averaged reaction rate in the first 5 min at a rotation speed of 400 r.p.m.

The results of the CHG reaction rate are shown in Figure 1. The reaction rate under mechanochemical conditions reached up to 117,000  $\mu\text{l g}^{-1} \text{s}^{-1}$  at a container temperature of 40 °C, which is 4 orders of magnitude higher than that under traditional thermal conditions at 600 °C (5  $\mu\text{l g}^{-1} \text{s}^{-1}$ ). Besides the increase in reaction rate, the reaction temperature was also dramatically reduced. In the thermal method, the hydrogasification reaction needs to be ignited above 450 °C. In contrast, with the mechanochemical method, the reaction can proceed even at ambient temperature (25 °C). This raises several questions: Why is the reaction initiated at such a low temperature, and why is the reaction rate enhanced so much?

It is likely that the extreme leap in performance stems from some unique properties of the mechanochemical process. To reveal the underlying physical nature of this process, we conducted a control experiment, which combined the mechanochemical method and the thermal method. We first activated the catalyst and carbon reactant *via* mechanochemical ball-milling. Then, after carefully transferring the sample into a fixed-bed reactor without air exposure, we hydrogenated the mechanochemically activated mixture using the standard thermal method.

The control result (yellow curve) is shown in Figure 1. The mechanochemically activated sample in the control experiment exhibited medium-level activity compared to the mechanochemical method and the thermal method. Unexpectedly, the mechanochemically activated samples were so reactive that the CHG occurred spontaneously, even without any heating, at a room temperature of 22 °C. The reaction rate was 0.051  $\mu\text{l g}^{-1} \text{s}^{-1}$ , which is comparable to the one observed with the physically-mixed samples at 500 °C (0.055  $\mu\text{l g}^{-1} \text{s}^{-1}$ ) in the thermal method. This result indicates that the ball-milling pretreatment can generate some reactive carbon species, which can easily be hydrogenated into hydrocarbons. Those reactive carbon species are created by the comminution due to mechanical movements, such as colliding and sliding.

In the complete CHG process, the bulk carbon first needs to be dissociated (carbon dissociation step), then the dissociated carbon atoms are hydrogenated into hydrocarbons (hydrogenation step). The spontaneous hydrogasification of reactive carbon species determines that the hydrogenation step in CHG is not a rate-determining step (RDS). Consequently, the carbon dissociation is the RDS in the CHG.<sup>[10]</sup>

Noticeably, the activity of the mechanochemically activated sample dropped drastically once the temperature surpassed 525 °C. This is attributed to the fast depletion of reactive carbon species and the debonding between the catalysts and carbon materials. This suggests that a continuous supply of reactive carbon species is crucial to maintain a high reaction rate in the solid-gas reaction.

This brings us to the second question: why is the reaction rate using the mechanochemical method higher than that in the control experiment? In the mechanochemical method, the mechanical movements can continuously and simultaneously activate both the carbon materials and the Co catalyst *via* external mechanical force (Figure 2a). This ensures that the catalyst is always in intimate contact with the carbon materials.<sup>[18]</sup> This factor guarantees that CHG occurs at a high rate without interruption. In addition, the high-density defects are also thought to facilitate the carbon dissociation and violent collisions can accelerate the desorption of intermediate hydrocarbon species (Figure 2b).

To substantiate these assumptions, density functional theory (DFT) calculations were carried out. During carbon dissociation, dissociating a C atom from its sextet ring requires cleaving two conjugated C-C bonds, which requires at least 7.4 eV ( $I_1$  in Figure 2b, c, Figure S7). Even the breaking of a C bond at a dangled Klein edge requires 3.8 eV ( $I_2$  in Figure 2b, c, Figure S7). Those energies are much higher than the energy barrier (0.9 eV, Figure S8) in the hydrogenation step. This further verifies that the carbon dissociation is the RDS.

Now the RDS—carbon dissociation—will be discussed in more detail. In our method, carbon can be dissociated into free carbons in two ways: by direct mechanical cracking, and indirectly, with the help of a catalyst. The mechanical cracking results from ball-milling comminution, which can even amorphize the sample with repeated mechanical movements.

The DFT calculations confirmed that proximity between the Co catalyst and carbon was necessary. Although the Co catalyst can decrease the total dissociation energy, when the carbon is not close the Co ( $II_1$  and  $II_2$  in Figure 2b, c, Figure S7) the energy barriers are still practically the same as in the catalyst-free case.

When the carbon comes into contact with the Co(111) extended surface, the energy barrier can be dramatically reduced, from 7.4 eV to 2.3 eV ( $III_1$  in Figure 2b, c). However, this is still too high for the reaction to go smoothly. It is known that mechanochemically activated solid materials lie in a non-equilibrium state, where a high density of structural defects can lower the effective energy barrier of the reaction.<sup>[19]</sup> The DFT calculation indicated that the energy barrier can further decline, to 0.6 eV, when defects are present in both the catalyst and carbon ( $III_2$  in Figure 2b, c).

Once the free carbon atoms are adsorbed on the surface of the catalyst, the Co–C bonds are so strong that the

catalyst surface can even be reconstructed, and a thin Co carbide layer will be formed. In the reaction process, carbide intermediates are dynamically formed and depleted. Our DFT results (Figure S8, S9) determined that pure cobalt carbide ( $\text{Co}_3\text{C}$ , 1.0 eV) could have an enhanced activity relative to the one of face centered cubic (*fcc*) Co (1.3 eV). When cobalt carbides are formed on the top surface of Co (near surface carbide model), the activity can be further increased (energy barrier, 0.9 eV), which agrees with reports on the Fischer–Tropsch process.<sup>[20,21]</sup> The impact energy is so rapidly released during milling that the lattice parameters and atom positions do not have enough time to fully relax. A portion of the mechanical energy (usually around 1.0 eV) can be directly transferred to the adsorbed species,<sup>[11,22]</sup> thus allowing the hydrogenation step to easily proceed under collisions.

The mechanochemical method not only enhances activity, but also improves selectivity at low temperature.<sup>[23]</sup> Using the thermal method,  $\text{CH}_4$  yields are usually low (80% at thermodynamic equilibrium at 600 °C). Using our method, the  $\text{CH}_4$  selectivity reached up to 99.78%, with 0.22%  $\text{C}_2\text{H}_6$  and 0.001% remnant  $\text{H}_2$  as byproducts (Figure S10). That is to say, the maximum conversion ratio of  $\text{H}_2$  can reach as high as 99.999%. The calculated energy barrier of  $\text{C}_2\text{H}_6$  is quite high (2.7 eV, Figure S11), making the formation of  $\text{C}_2\text{H}_6$  very hard at low temperature, a result of narrowing the Boltzmann distribution.<sup>[24]</sup> The lower remnant of  $\text{H}_2$  is mainly related to the fact that CHG is an exothermic reaction and, according to Le Chatelier’s principle<sup>[25]</sup>, low temperature facilitates the reaction in a forward direction. Besides high selectivity, the CHG also exhibited high cycle stability (Figure S12).

To determine the reactive carbon species and reaction mechanism, a series of elaborate characterizations were conducted. The mechanochemically processed samples exist in a thermodynamically unstable state, caused by the high-density defects. Thus, when exposed to air, the sample oxidizes quickly (Movie S1). To obtain reliable characterizations, all the measurements were conducted in air-free environments during the entirety of the process.

Extended X-ray absorption fine structure (EXAFS) is a technique for studying local atomic structures. The EXAFS-derived radial distribution function (RDF) directly informs about bonding. As shown in Figure 3a, Co–C bonds located at 1.3 Å are formed as a result of the reaction. The chemical states were studied *via* high resolution photoemission spectroscopy (PES) and X-ray absorption near edge structure (XANES). Both the C 1s core level spectrum (Figure S13a) and the C K-edge XANES (Figure S13b) established the existence of cobalt carbides. Here however, the Co L-edge XANES cannot provide useful information (Figure S13c), because it is difficult to distinguish different cobalt species with high resolution.

At this point, the techniques mentioned above can only prove that cobalt carbides were present during hydrogasification, but the types of carbides cannot be determined. The X-ray powder diffraction (XRD, Figure 3b) patterns show that some of  $\text{Co}_3\text{C}$  carbides may have been involved in hydrogasification. The broad and weak peaks

indicate poor crystallinity because of the high-density of defects. Since XRD is not sensitive to short-range ordered phases, more accurate characterizations were needed.

Here, we resorted to a more appropriate technique—solid state nuclear magnetic resonance (NMR) to analyze Co coordination environments at short-range. Since Co metal is ferromagnetic, no external static magnetic field needs to be applied, and the internal field (IF) of the metal itself is sufficient to lift the degeneracy of the nuclear spin levels. The IF-NMR in Figure 3c shows a main resonance at 214 MHz assigned to  $^{59}\text{Co}$  in *fcc* structure.<sup>[26]</sup> The broadened *fcc* Co peak demonstrated that the catalyst was nanosized, or largely amorphized because of a high-density of defects. This observation agrees well with the XRD. The formation of  $\text{Co}_3\text{C}$  was established by a  $^{59}\text{Co}$  well-marked resonance at 75 MHz.<sup>[27]</sup> In addition, IF-NMR showed that some of the carbon atoms were dissolved in the lattice of the *fcc* Co [Co(C) solid solution, between about 150 and 200 MHz]. The resonance frequency of the solid solution was very broad, reflecting the distribution of the number of carbon atoms in Co nearest neighbor (NN) coordination shell. The IF-NMR of the Co catalyst after hydrogenation determined that the  $\text{Co}_3\text{C}$   $^{59}\text{Co}$  resonance disappeared (Figure S14a) and that only minor amounts of carbon solid solutions were left. This was further verified by XRD (Figure S14b). The results were consistent with the fact that nearly 100% of the initial carbon atoms were converted into hydrocarbons.

To further verify the occurrence of carbides, a  $^{13}\text{C}$ -labeled experiment was performed to directly check the Co-C coordination by IF-NMR measurement (Figure 3d, Note S1). A new signal around 6.5 MHz appeared in the sample obtained from a  $^{13}\text{C}$ -labeled source. Because this new signal was not observed in samples obtained from non- $^{13}\text{C}$ -labeled carbon sources, it has a strong likelihood to be due to the resonance of  $^{13}\text{C}$  in the local field of Co. Therefore, this supported the presence of cobalt-carbon compounds, major  $\text{Co}_3\text{C}$  and/or minor Co(C) solid solution. As discussed in the DFT results, carbides are commonly regarded to be a pivotal intermediate for CHG.<sup>[20,21,28]</sup>

In summary, the extreme improvement in CHG performance at low temperature can be attributed to the unique properties of mechanochemistry. These properties include the following four aspects. (I) Mechanical movements, especially colliding and sliding, can facilitate carbon dissociation *via* direct cracking. (II) The mechanical movements can continuously activate both the carbon materials and the catalyst, and ensure the catalyst remains in intimate contact with the carbon materials.<sup>[18]</sup> This point is very important for the solid-gas reaction. (III) The induced high-density defects, which possess high energy in a thermodynamically nonequilibrium state, can accelerate the carbon dissociation *via* energy compensation. (IV) The violent collisions can transfer partial mechanical energy to the adsorbed carbon intermediates, facilitating hydrocarbon generation.<sup>[29]</sup>

To prove our method can easily be scaled-up, a larger scale experiment was carried out on a roll-mill. Indeed, roll-mill is relatively easy to scale-up to tonnage quantities of materials, for various applications.<sup>[30]</sup> The charcoal was

first prepared *via* pine wood pyrolysis in a leakage-free furnace (Figure 4a). The as-prepared charcoal was loaded into a home-made roll-mill with a container size of 15 liters (Figure 4b, Movie S2). First, a blank experiment was conducted to rule out the contamination of carbon solid solution in the steel. Our experimental result determined that only a trace of CH<sub>4</sub> could be generated (Figure S15).<sup>[12]</sup> Compared to a planetary mill, the roll-mill releases much less energy, which has a big influence on the reaction rate. To fairly compare the two different methods, we used the generated CH<sub>4</sub> per kilowatt hour (kWh) as an indicator. As shown in Figure 4c, the large-scale roll-mill displayed a CH<sub>4</sub> yield similar to the small-scale planetary mill.

### **Conclusion:**

Our work introduces a new method for carbon hydrogasification, with high rates at low temperature. The synthesized hydrocarbons are carbon-neutral. Consequently, the all cycle, from biomass production to mechanochemical CHG and finally methane utilization is a net-zero carbon dioxide emission process and might even be partially net-negative. This is an important prospect to replace the limited carbon-positive natural gas reserves,<sup>[9,31,32]</sup> and to prevent global warming. In addition, our findings can be used as a non-oxidative method to regenerate coke-poisoned catalysts, which is frequently required in large-scale industrial production. This method not only avoids aggregation when burning the carbon due to the highly exothermic nature of the reaction,<sup>[33]</sup> but also reduces the catalyst size at the same time.

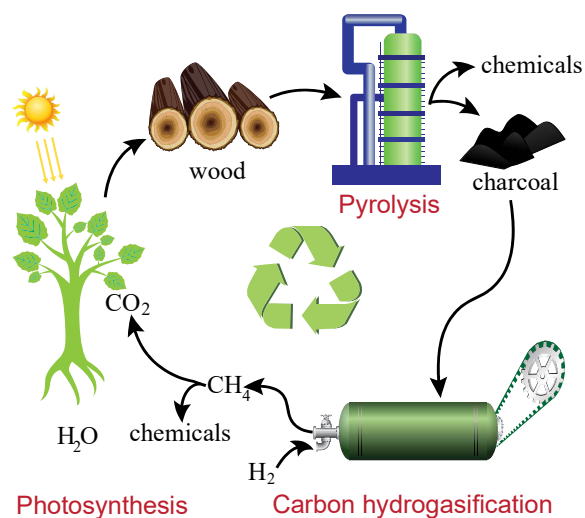
### **Acknowledgements:**

We are grateful for the use of the Pohang Accelerator Laboratory (8C beamline, South Korea). This work was supported by the Creative Research Initiative (CRI, 2014R1A3A2069102), and Science Research Center (SRC, 2016R1A5A1009405) programs through the National Research Foundation (NRF) of Korea, and the U-K Brand Project (1.200096.01) of UNIST. NMR equipment at ESPCI Paris is funded in part by the Paris Region. This project has received funding from the European Union's Horizon 2020 research and innovation programme under the Marie Skłodowska-Curie grant agreement No 754387.

**Keywords:** mechanochemistry • hydrogenation • methane • carbon-neutral • solid-gas reaction

- [1] P. Basu, *Biomass Gasification, Pyrolysis and Torrefaction*, Elsevier Inc., London, **2013**.
- [2] J. Zhang, L. Wang, B. Zhang, H. Zhao, U. Kolb, Y. Zhu, L. Liu, Y. Han, G. Wang, C. Wang, D. S. Su, B. C. Gates, F.-S. Xiao, *Nat. Catal.* **2018**, *1*, 540–546.
- [3] D. C. Elias, R. R. Nair, T. M. G. Mohiuddin, S. V. Morozov, P. Blake, M. P. Halsall, A. C. Ferrari, D. W. Boukhvalov, M. I. Katsnelson, A. K. Geim, K. S. Novoselov, *Science* **2009**, *323*, 610–613.
- [4] F. Zhang, M. Zeng, R. D. Yappert, J. Sun, Y. H. Lee, A. M. LaPointe, B. Peters, M. M. Abu-Omar, S. L. Scott, *Science* **2020**, *370*, 437–441.
- [5] K. J. Hüttinger, P. Schleicher, *Fuel* **1981**, *60*, 1005–1012.
- [6] G. Kyriakou, M. B. Boucher, A. D. Jewell, E. A. Lewis, T. J. Lawton, A. E. Baber, H. L. Tierney, M. Flytzani-Stephanopoulos, E. C. H. Sykes, *Science* **2012**, *335*, 1209–1212.
- [7] D. L. Trimm, *Catal. Rev.* **1977**, *16*, 155–189.
- [8] H. M. Torres Galvis, J. H. Bitter, C. B. Khare, M. Ruitenbeek, A. I. Dugulan, K. P. de Jong, *Science* **2012**, *335*, 835–838.
- [9] P. L. Walker, F. Rusinko, L. G. Austin, *Adv. Catal.* **1959**, *11*, 133–221.
- [10] W. Holstein, *J. Catal.* **1981**, *72*, 328–337.
- [11] G.-F. Han, F. Li, Z.-W. Chen, C. Coppex, S.-J. Kim, H.-J. Noh, Z. Fu, Y. Lu, C. V. Singh, S. Siahrostami, Q. Jiang, J.-B. Baek, *Nat. Nanotechnol.* **2021**, *16*, 325–330.
- [12] S. Reichle, M. Felderhoff, F. Schüth, *Angew. Chem. Int. Ed.* **2021**, *60*, 26385–26389.
- [13] E. Aneghi, V. Rico-Perez, C. de Leitenburg, S. Maschio, L. Soler, J. Llorca, A. Trovarelli, *Angew. Chem. Int. Ed.* **2015**, *54*, 14040–14043.
- [14] P. Baláž, M. Achimovicová, M. Baláž, P. Billik, C. Z. Zara, J. M. Criado, F. Delogu, E. Dutková, E. Gaffet, F. J. Gotor, R. Kumar, I. Mitov, T. Rojac, M. Senna, A. Streletskii, W. C. Krystyna, *Chem. Soc. Rev.* **2013**, *42*, 7571–7637.
- [15] G.-F. Han, F. Li, A. I. Rykov, Y.-K. Im, S.-Y. Yu, J.-P. Jeon, S.-J. Kim, W. Zhou, R. Ge, Z. Ao, T. J. Shin, J. Wang, H. Y. Jeong, J.-B. Baek, *Nat. Nanotechnol.* **2022**, DOI 10.1038/s41565-022-01075-7.
- [16] A. Tomita, Y. Tamai, *J. Catal.* **1972**, *27*, 293–300.
- [17] T. M. Gür, R. A. Muggins, *Science* **1983**, *219*, 967–969.
- [18] H. Jin, S. Xin, C. Chuang, W. Li, H. Wang, J. Zhu, H. Xie, T. Zhang, Y. Wan, Z. Qi, W. Yan, Y. R. Lu, T. S. Chan, X. Wu, J. B. Goodenough, H. Ji, X. Duan, *Science* **2020**, *370*, 192–197.
- [19] G. A. Somorjai, D. W. Blakely, *Nature* **1975**, *258*, 580–583.
- [20] M. Rahmati, M. S. Safdari, T. H. Fletcher, M. D. Argyle, C. H. Bartholomew, *Chem. Rev.* **2020**, *120*, 4455–4533.
- [21] Y.-P. Pei, J.-X. Liu, Y.-H. Zhao, Y.-J. Ding, T. Liu, W.-D. Dong, H.-J. Zhu, H.-Y. Su, L. Yan, J.-L. Li, W.-X. Li, *ACS Catal.* **2015**, *5*, 3620–3624.
- [22] F. Abild-Pedersen, J. Greeley, F. Studt, J. Rossmeisl, T. R. Munter, P. G. Moses, E. Skúlason, T. Bligaard, J. K. Nørskov, *Phys. Rev. Lett.* **2007**, *99*, 016105.
- [23] K. Kubota, Y. Pang, A. Miura, H. Ito, *Science* **2019**, *366*, 1500–1504.
- [24] J. M. Andersen, J. Mack, *Chem. Sci.* **2017**, *8*, 5447–5453.
- [25] G. Marnellos, M. Stoukides, *Science* **1998**, *282*, 98–100.
- [26] A. S. Andreev, J.-B. D’Espinose De Lacaillerie, O. B. Lapina, A. Gerashenko, *Phys. Chem. Chem. Phys.* **2015**, *17*, 14598–14604.
- [27] K. Hiraoka, A. Oota, H. Jinushi, *J. Phys. Soc. Japan* **2008**, *77*, 75–77.
- [28] J. G. McCarty, H. Wise, *J. Catal.* **1979**, *57*, 406–416.
- [29] A. P. Amrute, Z. Łodziana, H. Schreyer, C. Weidenthaler, F. Schüth, *Science* **2019**, *366*, 485–489.
- [30] P. Balaz, *Mechanochemistry in Nanoscience and Minerals Engineering*, Springer-Verlag, Berlin, Heidelberg, **2008**.
- [31] M. Cargnello, J. J. D. Jaen, J. C. H. Garrido, K. Bakmutsky, T. Montini, J. J. C. Gamez, R. J. Gorte, P. Fornasiero, *Science* **2012**, *337*, 713–717.
- [32] T. Li, Y. Yao, Z. Huang, P. Xie, Z. Liu, M. Yang, J. Gao, K. Zeng, A. H. Brozena, G. Pastel, M. Jiao, Q. Dong, J. Dai, S. Li, H. Zong, M. Chi, J. Luo, Y. Mo, G. Wang, C. Wang, R. Shahbazian-Yassar, L. Hu, *Nat. Catal.* **2021**, *4*, 62–70.
- [33] J. L. Figueiredo, D. L. Trimm, *J. Catal.* **1975**, *40*, 154–159.

## Entry for the Table of Contents



Plants capture  $\text{CO}_2$  from the air and fix it with  $\text{H}_2\text{O}$  into carbohydrate molecules *via* photosynthesis. The main photosynthesized biomass—wood can be converted into charcoal and chemicals *via* pyrolysis. The charcoal can then be hydrogenated into hydrocarbons using a mechanochemical method. The produced  $\text{CH}_4$  can be used directly as fuel, or as feedstock for the synthesis of other chemicals. The whole carbon cycle would be neutral or negative.

## Figures

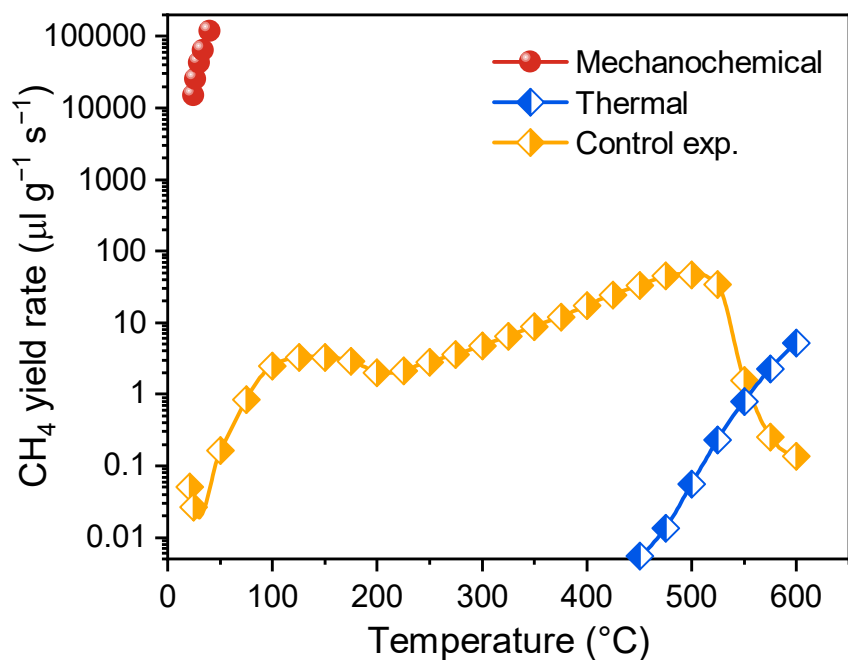


**Figure 1 | Carbon hydrogasification reaction under different conditions.** The red curve indicates the mechanochemical method, in which carbon hydrogasification is driven by ball-milling. The temperature used in the mechanochemical method is the container temperature, which increased due to mechanical collision during the ball-milling. In the thermal method (blue curve), the reaction is carried out on a fixed-bed reactor, with nanosized catalysts physically mixed with carbon black. In the control experiment (yellow curve), the catalyst and carbon black were first mechanically activated by ball-milling, then the hydrogenation of the mixture was carried out on a fixed bed reactor. In all the experiments, the catalyst was Co, and the solid carbon was carbon black.

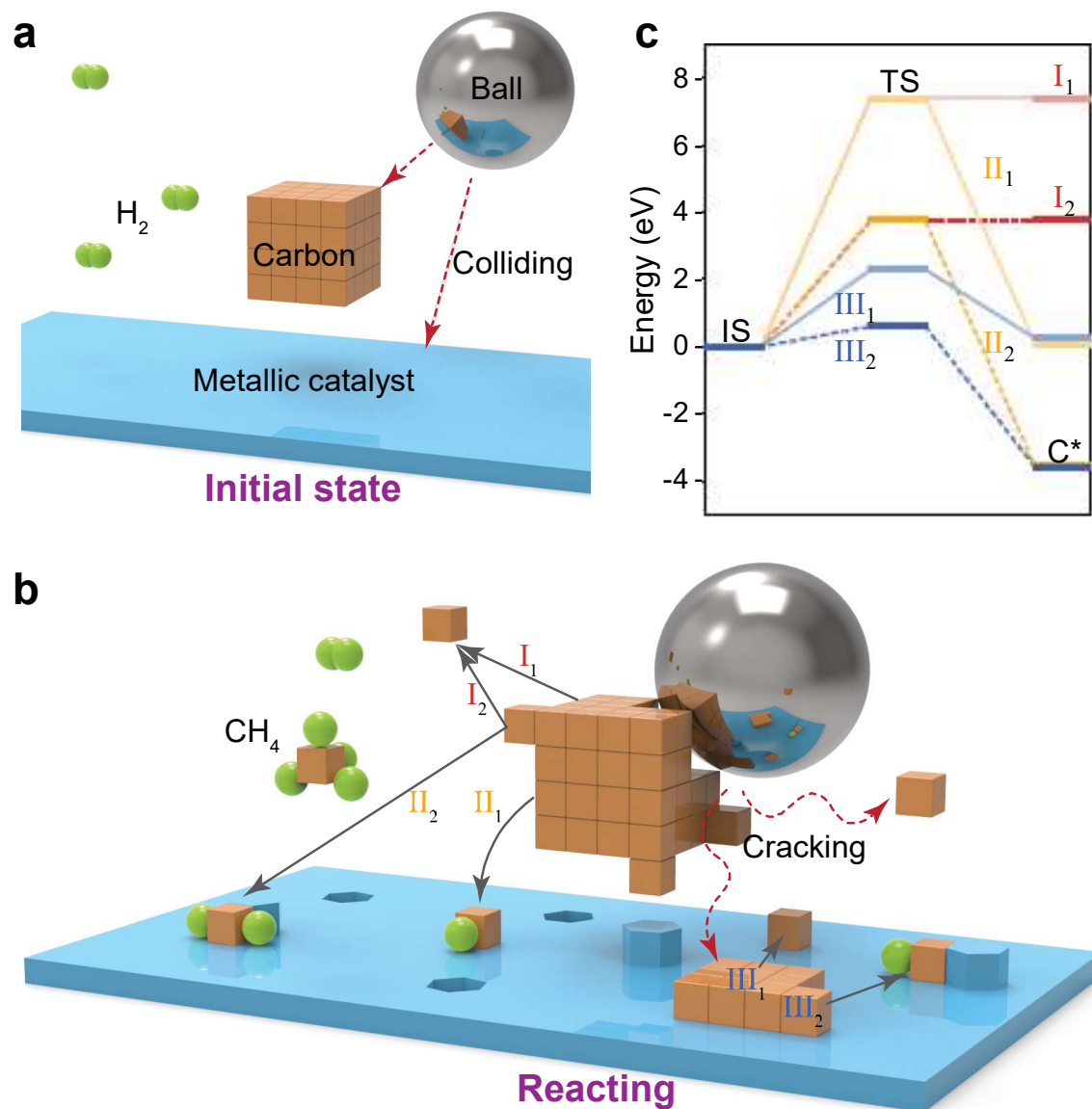


**Figure 2 | Carbon hydrogasification reaction mechanism under mechanochemical conditions.** a, Mechanical collisions simultaneously reduce the Co catalyst and carbon to nanosize and activate them. b, Carbon dissociation pathway and subsequently hydrogenation scheme. I, Carbon dissociation without catalyst. II, Carbon dissociation when the carbon does not contact the Co catalyst. III, Carbon dissociation when the carbon debris intimately contacts the Co catalyst. The superscripts 1 and 2 stand for the defect-free model (dissociating one carbon atom via breaking two conjugated C-C bonds) and the defect model (one Klein C-C bond on the edge), respectively. When the Co catalyst is present, superscripts 1 and 2 additionally correspond to the Co(111) extended surface and defects, respectively. c, Energy profiles of carbon dissociation based on DFT calculations, where IS and TS stands for initial state and transition state, respectively.

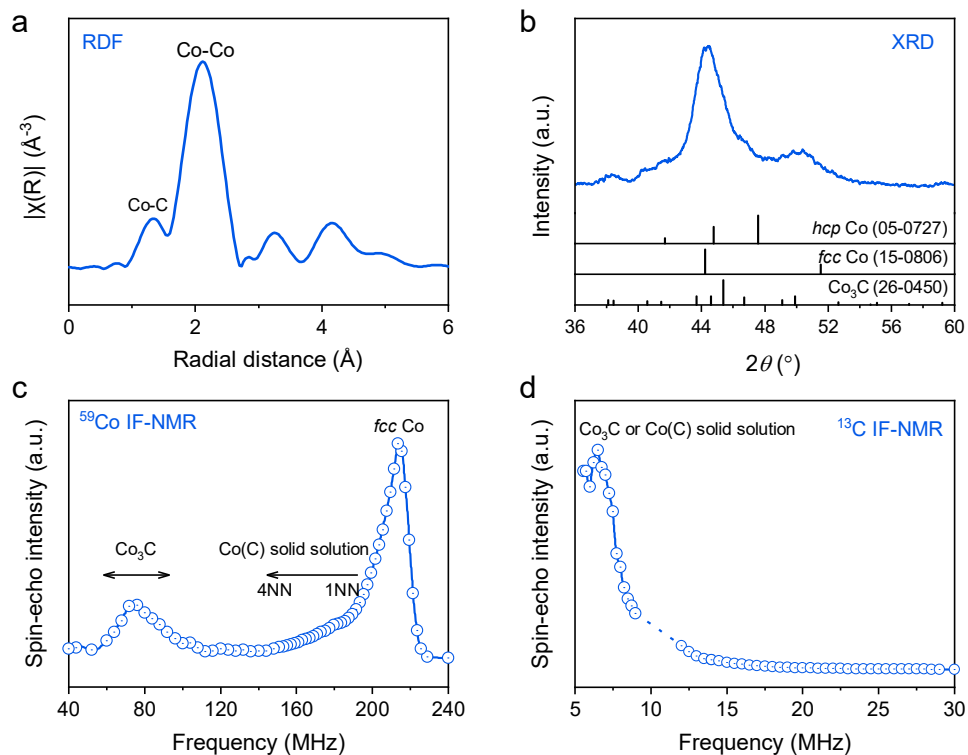


**Figure 3 | Structure characterizations.** a) Radial distribution function (RDF), derived from extended X-ray absorption fine structure (EXAFS). b) X-ray diffraction pattern (XRD). c)  $^{59}\text{Co}$  internal field nuclear magnetic resonance (IF-NMR). NN, nearest neighbor. d)  $^{13}\text{C}$  IF-NMR, measured under the internal field of the Co. The experimental setup cannot measure data between 9 and 12 MHz (dashed line). The sample used for  $^{13}\text{C}$  NMR was fully labeled with  $^{13}\text{C}$

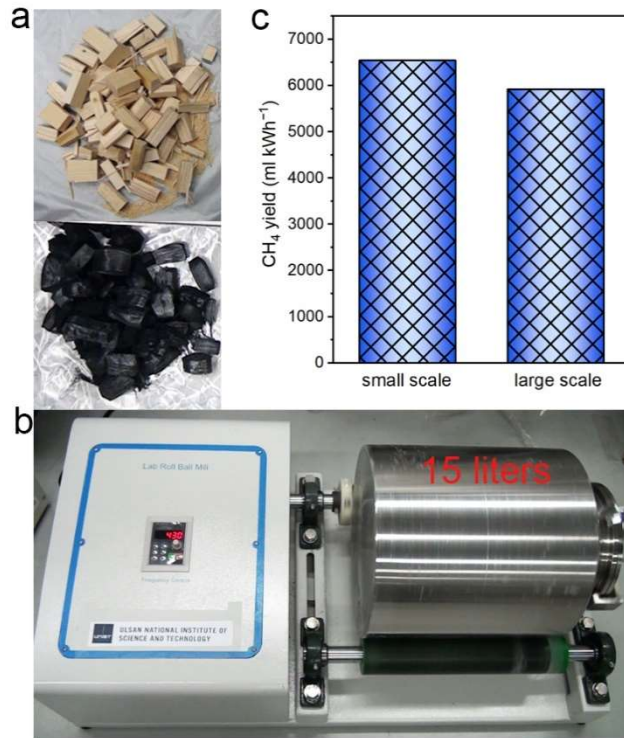


**Figure 4 | Large scale carbon hydrogasification.** a) Pine wood (top), and as-prepared charcoal after wood pyrolysis (bottom). b) Home-made roll-mill with a 15-liter container. c) Comparison between small-scale planetary mill and large-scale roll-mill.